Stem Cell Reports
Report

ISSCR

OPEN ACCESS

Dermatopontin in Bone Marrow Extracellular Matrix Regulates Adherence but Is Dispensable for Murine Hematopoietic Cell Maintenance

Ashley C. Kramer,[1] Amanda L. Blake,[1] Mandy E. Taisto,[1] Michael J. Lehrke,[1] Beau R. Webber,[1,2] and Troy C. Lund[1,*]

[1]Department of Pediatrics, Blood and Marrow Transplant Program, University of Minnesota Medical School, MMC 366, 420 Delaware Street SE, Minneapolis, MN 55455, USA

[2]B-MoGen Biotechnologies, Inc., 614 McKinley Place NE, Minneapolis, MN 55413, USA

*Correspondence: lundx072@umn.edu

http://dx.doi.org/10.1016/j.stemcr.2017.07.021

SUMMARY

The hematopoietic marrow microenvironment is composed of multiple cell types embedded in an extracellular matrix (ECM). We have explored marrow ECM using mass spectrometry and found dermatopontin (DPT), a small non-collagenous ECM protein, to be present. We found that DPT cooperates with other ECM proteins to promote hematopoietic cell adherence *in vitro* on plastic as well as OP9 stromal cells. We generated constitutional DPT$^{-/-}$ mice that were viable and had no peripheral lympho-hematopoietic abnormalities. The composition of the marrow of wild-type and DPT$^{-/-}$ mice was equivalent in terms of cellularity, CFU-C, LSK (Lineage^{-}, SCA-1^{+}, KIT^{+}), and LSK-SLAM (LSK, CD48^{-}, CD150^{+}) frequencies. These data suggest that DPT fosters adherence but is not required for steady-state hematopoiesis *in vivo*. There are likely overlapping cellular adhesion mechanisms that can compensate to maintain the hematopoietic niche in the absence of DPT.

INTRODUCTION

The bone marrow niche is composed of hematopoietic cells, non-hematopoietic cells (endothelial cells, stromal cells, adipocytes, etc.), and an extracellular matrix (ECM). The ECM is comprised of various structural proteins (most prevalent are collagen species), non-collagenous proteins, and associated growth factors. Many components of the ECM have been shown to be critically important for the growth and development of hematopoietic ontogeny. For example, tenascin, a 214 kDa marrow glycoprotein, has been shown to be significant in the maintenance of activity of hematopoietic colony-forming unit cell (CFU-C) in marrow, as well as to assist in hematopoietic cell and progenitor (HSPC) longevity (Forsberg et al., 1996; Ohta et al., 1998). Fibronectin has been shown to be important both for cellular adhesion and for proliferation of erythroid and primitive hematopoietic progenitors *in vitro* (Weinstein et al., 1989). Alternatively, the defense collagen, adiponectin, has been shown to negatively regulate the expansion of myelomonocytic cells *in vitro*, as well as to inhibit macrophage phagocytosis (Yokota et al., 2000).

It has been reported recently that the ECM-related protein dermatopontin (DPT) is important in HSPC maintenance during *ex vivo* culture expansion on AFT024 stromal cells. This phenomenon is hypothesized to occur by allowing HSPC to maintain closer contact with the stroma. Through a mass-spectrometry-based interrogation of decellularized murine bone marrow, we have identified DPT to be a component of the ECM and show that it can promote cellular adherence. We generated a mouse with a constitutional deletion in *Dpt;* it did not reveal any lympho-hematopoietic defects during development or at steady state, but interestingly was able to mobilize peripheral CFU-C more efficiently with AMD3100. These data suggest that DPT may play a role in HSPC adhesion, but is not required for intrinsic hematopoiesis.

RESULTS

To evaluate marrow ECM composition for proteins that play a role in hematopoietic cell behavior, we decellularized murine femurs (Figures 1A–1E) (Price et al., 2010). The decellularization process uses the sequential application of detergents to disrupt cells and remove the majority of the intracellular material. The underlying extracellular matrix scaffold remains intact, indicated by fluorescent eosin staining and scanning electron microscopy (Figures 1E, 1F, and S1). After solubilzation of the enduring ECM proteins, we performed protein identification using tandem mass spectrometry. We identified 240 individual protein species, ranging in size from 56 to 35,213 amino acids (Figure 1G). Examples of identified proteins included titin, several collagen species, fibrinogen, biglycan, vitronectin, and fibrillin-1. Also present were prevalent residual cellular proteins, including myosin, actin, and histone species. Ontogeny examination using PANTHER GO term analysis for "Molecular Function" showed the majority of the proteins to be involved with "binding," have structural activity, or have catalytic activity (43.4%, 29.7%, and 18.5%, respectively) (Figure 1H). Similar analysis for shared "Pathways"

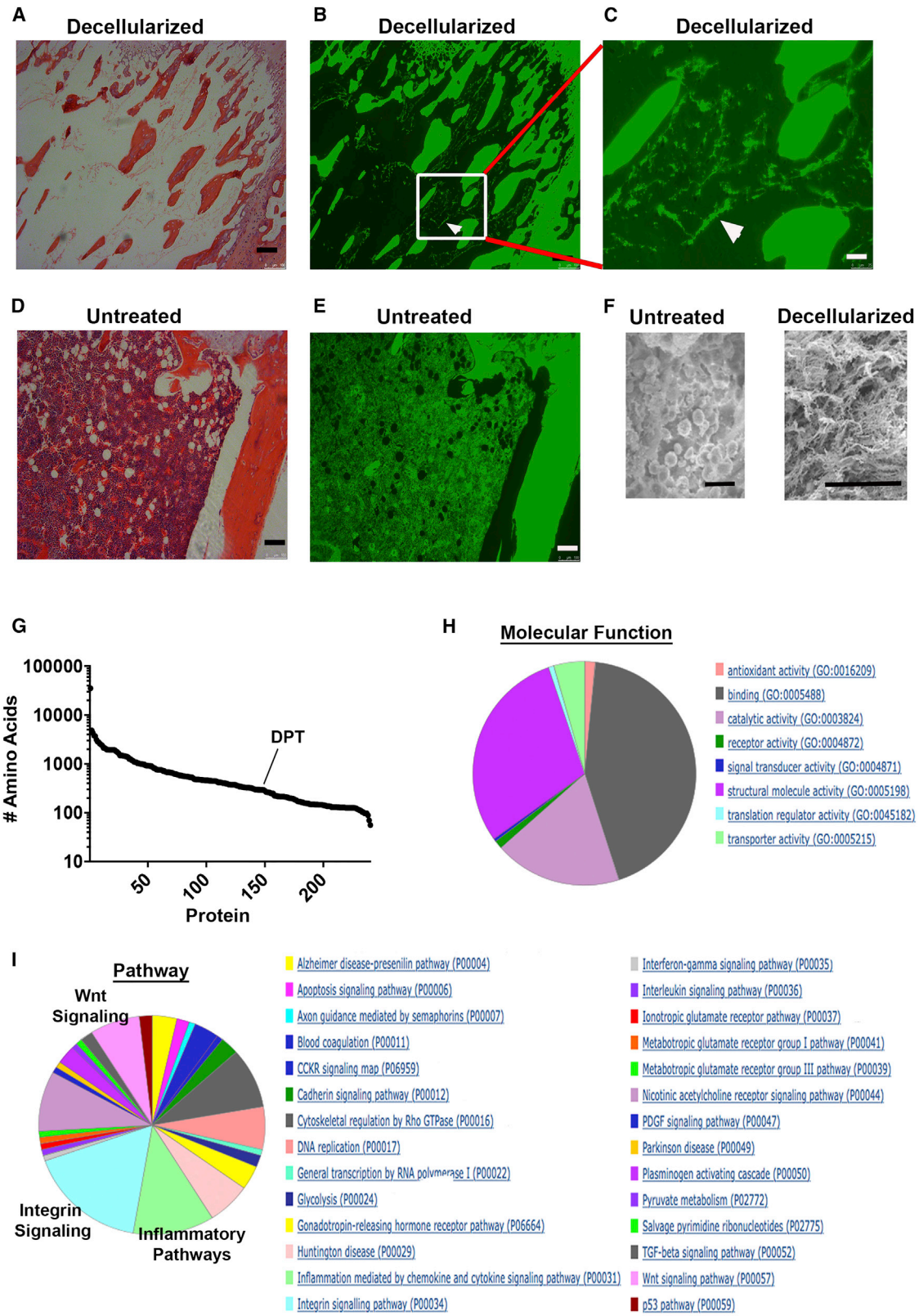

(legend on next page)

indicated that many of the ECM proteins were involved in integrin signaling, inflammatory signaling, or Wnt signaling (17.0%, 11.6%, and 7.1%, respectively) (Figure 1I).

In the ECM, we detected DPT, a 201 amino acid (24 kDa) ECM-related protein that has been shown to interact with collagen, fibronectin, and decorin (Okamoto et al., 1996, 1999, 2010) and is also found in the peripheral circulation associated with fibrin (Wu et al., 2014). Historically, DPT had not been shown to play a role in the bone marrow microenvironment, although recently it has been demonstrated that DPT can promote the *ex vivo* expansion of murine HSPC with speculation that it promotes adhesion of HSPC to stroma (Kokkaliaris et al., 2016). Therefore, we assessed the ability of whole bone marrow (WBM) cells to adhere to various ECM proteins in the presence of DPT. Using ECM arrays, we found that DPT could significantly promote adherence of murine WBM in the presence of collagen IV, laminin, tenascin, vitronectin, fibronectin, and retronectin (Figures 2A and 2B).

To promote *ex vivo* HSPC expansion, it was thought that DPT interacted with HSPC and the stromal matrix to encourage cell-to-cell contact (Kokkaliaris et al., 2016). We determined that fluorescently tagged DPT could physically bind WBM and LSK cells (Figures 2C–2E). We next tested if DPT could alter the ability of WBM or LSK to divide and differentiate into CFU-C *in vitro* and found no positive or negative effects (Figures 2F and 2G). When recombinant DPT (rDPT) was added to LSK expanded *ex vivo* using cytokines alone on plastic, we found no influence on cell expansion (Figure 2H, $p = 0.73$). On the contrary, LSK expanded on OP9 stromal cells (Nakano et al., 1994; Yoshida et al., 1990) demonstrated close to a 50% increase in the presence of rDPT (Figure 2H, $p = 0.003$). Not only were the numbers of LSK progeny increased, but we also measured a 46% increase in their adherence to the OP9 stroma (Figure 2I, $p = 0.03$). These data suggest a role of DPT in cellular adherence in *ex vivo* expansion. We tested the *in vivo* homing ability of culture-expanded LSK in lethally irradiated congenic mice. Sixteen hours after transplant, we found no difference in the homing ability of cultured expanded cells due to the addition of DPT (Figure 2J, $p = 0.37$). DPT is known to have secondary motifs including an N-terminal secretion signal, C-C bridge motifs, and a heparan-binding domain (Figure 2K) (Superti-Furga et al., 1993). It has been previously demonstrated that the addition of heparin, the chemically related glycosaminoglycan to heparin, can inhibit the pro-adherence function of DPT *in vitro* (Okamoto et al., 2010). When heparin was added to LSK expanded on OP9 with DPT, we found a 25% reduction in the numbers of LSK progeny generated and a reduction in cellular adherence (Figures 2H and 2I). Cumulatively, these data indicate that DPT plays a role in cellular adhesion in concert with other ECM proteins that can be attenuated by heparin.

We generated DPT knockout mice to explore the specific role of DPT in native hematopoiesis. The first exon of DPT was targeted using CRISPR guide RNA (gRNA) molecules that were injected along with Cas9 mRNA into single-cell zygotes. The initial founder was chosen based on a large (50 bp) deletion, causing a frameshift and generation of multiple downstream stop codons (Figure 3A); animals were out-crossed to generate stable lines. Immunoblot assay (Figure 3B) confirmed the absence of mature DPT in $DPT^{-/-}$ mice. $DPT^{-/-}$ mice were fertile, showed no overt phenotypic evidence of disease, and had a normal lifespan consistent with a previous report of $DPT^{-/-}$ mice created to study skin laxity (Takeda et al., 2002). We assessed total circulating white blood cell, neutrophil, lymphocyte, monocyte, hemoglobin, and platelet concentrations and found no differences between wild-type and $DPT^{-/-}$ mice. Unexpectedly, $DPT^{+/-}$ mice did show elevated numbers of neutrophils and lymphocytes compared with wild-type. We can only speculate that there may be downstream binding partners to DPT that could be altered in a DPT haploinsufficient state to promote some amount of white cell expansion (Figures 3C–3G). The frequencies of B220, Gr1, CD3, and T cell subsets in adult $DPT^{-/-}$ mice were comparable with those of wild-type (Figures 3H and 3I).

Figure 1. Decellularization of Murine Marrow and Mass Spectrometry Analysis of ECM

(A–E) H&E staining showing decellularized (A–C) and untreated (D and E) murine femurs (distal end). (B and C) The eosin fluorescent signal emitting from the ECM. The white arrowhead indicates the eosin-stained ECM left behind after decellularization. Micrographs taken at 100× (A–D) and 400× (E). Images taken on a Leica DMI 6000 microscope using bright field or the L5 fluorescence filter set (similar to fluorescein isothiocyanate fluorophore detection). Scale bars represent 100 μm.

(F) Scanning electron microscopy images from untreated and decellularized murine femurs. The untreated image contains evident small round hematopoietic cells, while the decellularized image show only underlying ECM. The scale bars represent 25 μm. See Figure S1 for lower magnification views.

(G) Amino acid sequence lengths of specific proteins identified by mass spectrometry in decellularized marrow.

(H) Top PANTHER GO term analysis for "Molecular Function" from murine marrow ECM proteins identified by mass spectrometry. See Table S1 for specific data.

(I) Top PANTHER GO term analysis for "Pathways" from murine marrow ECM proteins identified by mass spectrometry. See Table S2 for specific data.

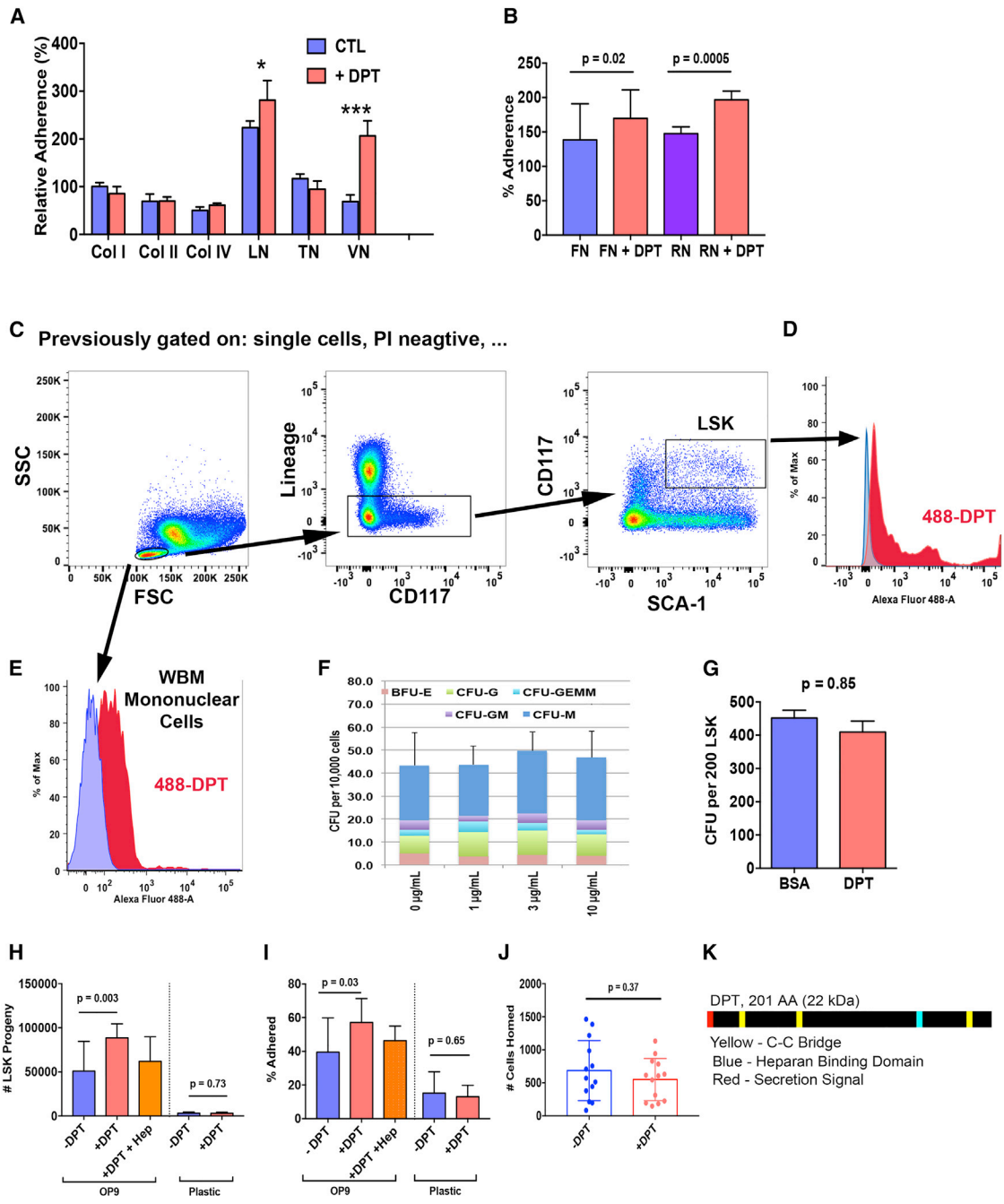

Figure 2. DPT Binds Hematopoietic Cells and Promotes Adherence

(A) WBM adherence to collagen (Col) species I–IV, laminin (LN), tenascin (TN), and vitronectin (VN) coated wells. 150,000 freshly isolated murine WBM cells were plated in media in a total volume of 100 µL. rDPT was added at 2 µg/well. After 1 hr at 37°C, the wells were washed three times. Adhered cells were quantified using Lysis/CyQuant GR fluorescent dye. Adhesion was normalized to Col I, n = 6 wells/condition, pooled data from three independent experiments shown. *$p < 0.05$, ***$p < 0.001$.

(B) Adhesion assay of murine WBM to wells coated with fibronectin (FN) or retronectin (RN) perform as in (A). Adhesion was normalized to FN, n = 6 wells/condition, pooled data from three independent experiments shown.

(C–E) rDPT was covalently labeled with Alexa Fluor 488 and incubated with WBM at 1 µg/mL for 60 min. Cells were washed with ice-cold PBS followed by flow cytometry. (C) Flow cytometry gate settings. (D) and (E) 488-DPT histogram plots for LSK and WBM mononuclear cells, respectively. Red plots show labeled DPT versus blue non-specific control (488-Fab′ fragment).

(legend continued on next page)

To determine if hematopoietic stress could reveal a phenotype in DPT$^{-/-}$ mice, we analyzed the ability of DPT$^{-/-}$ mice to recover from administration of 5-fluorouracil (5-FU). Figure 3J shows no significant difference in the peripheral WBC nadir or trajectory of recovery after 5-FU challenge. We also assessed marrow CFU-C just prior to peripheral count recovery (10 days after injection) (Grzegorzewski et al., 1994) and found equivalent colony numbers (Figure 3K, p = 0.19). These data suggest that DPT$^{-/-}$ hematopoietic cells do not have a cell-intrinsic defect.

We next analyzed the bone marrow of DPT$^{-/-}$ mice and found similar cellularity and CFU-C content (Figures 4A and 4B). There were no differences in spleen cell counts between the two groups (Figure 4C) or in the numbers of marrow LSK (p = 0.08), and LSK-SLAM (CD48^{-}CD150^{+} LSK) (p = 0.42) (Figures 4D–4F).

Given that DPT plays a role in cell adhesion, we explored whether or not DPT$^{-/-}$ mice might show differences when induced to mobilize HSPC to the periphery. After administration of AMD3100, we found that peripheral blood CFU-C were significantly increased in DPT$^{-/-}$ mice compared with wild-type (Figure 4G, 284 versus 194 CFU-C/0.5 mL, p = 0.02). These data suggest the DPT$^{-/-}$ mice can achieve normal steady-state hematopoiesis during development into adulthood, but DPT plays a unique role in cell adhesion with the marrow microenvironment.

DISCUSSION

Until recently, DPT has not had a role in hematopoiesis. By interrogating differential RNA expression between HSPC "supportive" AFT024 stromal cells versus HSPC "non-supportive" 2018 stromal cells, Kokkaliaris et al. (2016) determined *Dpt* was one of the genes expressed in the supportive cells. The 2018 stromal cells showed reduced levels of DPT and were less supportive of HSPC *ex vivo* unless supplemental DPT was added.

Our data suggest that DPT plays a direct role in cellular adhesion of HSPC in the *ex vivo* culture setting through direct binding of HSPC and stroma, but does not have inherent growth factor properties by itself. We show that DPT can cooperate with other ECM proteins, collagen IV, laminin, tenascin, vitronectin, fibronectin, and retronectin, to promote WBM binding to a plastic surface. These data are consistent with prior reports that have shown DPT can support the adhesion of keratinocytes and fibroblasts to plastic (Liu et al., 2013; Okamoto et al., 2010). ECM proteins have previously been shown to play a role in hematopoiesis. For example, data from more than 20 years ago showed tenascin to be an important cytoadhesive ECM component for hematopoietic cells in the marrow (Klein et al., 1993). Mice that constitutively lack tenascin have been shown to have reduced survival and poor hematopoietic recovery after sublethal irradiation (Nakamura-Ishizu et al., 2012). Similarly, both vitronectin and fibronectin are present in the marrow and have been shown to be important for cellular adherence (Hassan et al., 1997; Seiffert, 1996).

Previously, DPT$^{-/-}$ mice were generated by Takeda et al. (2002) to show DPT was important in skin collagen fibrillogenesis, and DPT$^{-/-}$ mice demonstrated a thin dermis and increased skin elasticity. No evaluation of the lympho-hematopoietic system was performed. We generated constitutively deleted DPT$^{-/-}$ mice through a CRISPR/Cas9 approach that produced fertile, viable mice. Our data showed no peripheral blood cell or marrow HSPC abnormalities, suggesting that DPT was not required for hematopoiesis during development or de novo. Furthermore, during 5-FU-induced stress hematopoiesis, we did not find

(F and G) CFU-C assay was performed using 10,000 WBM cells with increasing amounts of rDPT (F) or 200 sorted LSK cells in the presence of 1.5 μg/mL rDPT (G). CFU were enumerated after 14 days in culture. There was no significant difference between any treated group and the control group using a one-way ANOVA (F). Pooled data from three independent experiments are shown.

(H) OP9 cells were grown to 80% confluence in a 96-well plate and irradiated at 3,000 Gy 1 day prior to LSK seeding. 100 LSK were sorted by flow cytometry into each well of the 96-well plate containing StemSpan SFEM (STEMCELL Technologies), mSCF, mTPO, hFlt3, hIL6, and hIL11 ± 2 μg/mL rDPT for 5 days. After which, the hematopoietic cells in suspension, as well as those adhered to the stroma, were enumerated separately by flow cytometry (n = 12 wells/condition, one of three independent experiments shown).

(I) The percentage of total cells that were bound to the stromal layer in (H). In some experiments 10 units/mL heparin was added per well. Pooled data from three independent experiments are shown.

(J) To test homing ability, CD45.2-derived LSK were expanded as in (H). CD45.1 recipient mice were irradiated at 9 Gy 24 hr prior to transplant. Each mouse received the combined contents from six wells of expanded LSK cells. Sixteen hours post transplant, femurs were harvested and homed donor cells were enumerated by flow cytometry.

(K) DPT amino acid sequence codes for N-terminal secretion signal (red), three C-C bridges (yellow), and a heparan-binding domain (light blue).

All data are shown as means ± SD, p values in (A), (B), (G), and (J) are derived from a Student's t test comparing experimental group with control. p Values in (H) and (I) are derived from a one-way ANOVA and Tukey post hoc analysis between all groups; only the comparisons with $p < 0.05$ are indicated.

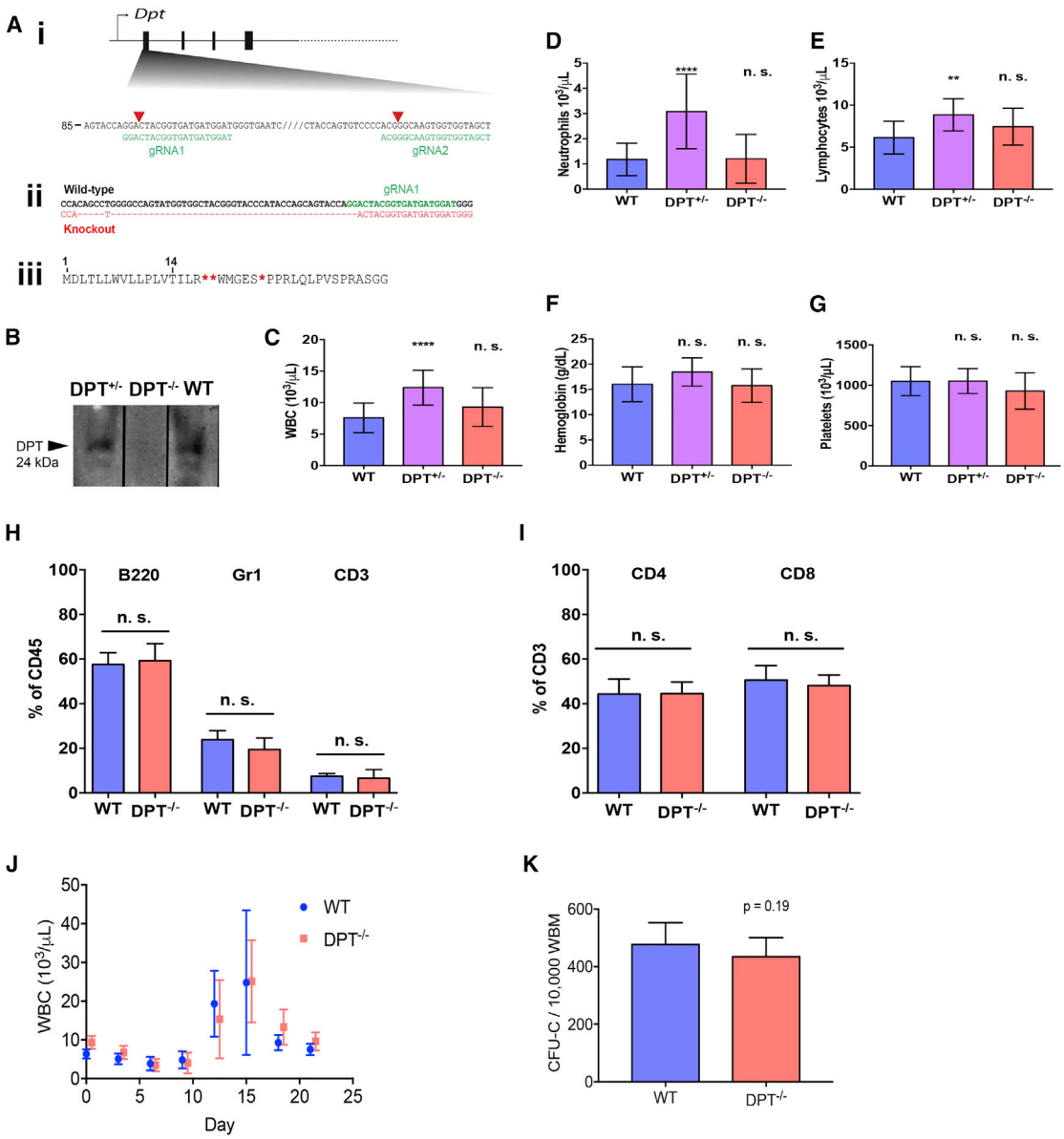

Figure 3. DTP Knockout Animals Have Normal Hematopoiesis

(A) (i) Targeted disruption of exon 1 of *mDpt* using CRISPR-Cas9. Base pair number refers to the coding sequence. Arrow indicates a transcriptional start site. Orange triangles indicate predicted cut sites. (ii) Wild-type (top) and founder $DPT^{-/-}$ (bottom) genome sequencing results indicate a deletion and subsequent frameshift. (iii) Predicted amino acid sequence from $DPT^{-/-}$ animals shows the last conserved amino acid at position 14, followed by deletion and frameshift, giving rise to multiple stop codons (red asterisks).

(B) Western blot of 10 μL of murine plasma from WT, $DPT^{+/-}$, $DPT^{-/-}$ mice.

(C–G) Blood counts were determined from 12-week-old mice via Hemavet analysis of peripheral blood (n = 12–14 individuals/group). ****p < 0.001, **p < 0.01, n.s., not significant, from one-way ANOVA and Tukey post hoc analysis comparing each group with the WT group. (C) Total white blood cell count; (D) neutrophil count; (E) lymphocyte count; (F) hemoglobin concentration; (G) platelet count.

(H) Flow cytometry of peripheral blood subsets from 12-week-old mice; data are shown as a percentage of CD45-positive cells (n = 12–14 individuals/group).

(I) Flow cytometry of $CD3^+$ subsets in the peripheral blood from 12-week-old mice; data are shown as a percentage of CD45-positive cells (n = 12–14 individuals/group).

(J) Mice were treated with 150 μg/kg 5-FU, and peripheral WBC was assessed every 3 days. There were no differences between the groups at any time point using Student's t test. (n = 10–12 individuals/group).

(K) Mice were treated with 150 μg/kg 5-FU and marrow CFU-C 10 days later. p Value is from a Student's t test (n = 10–12 individuals/group).

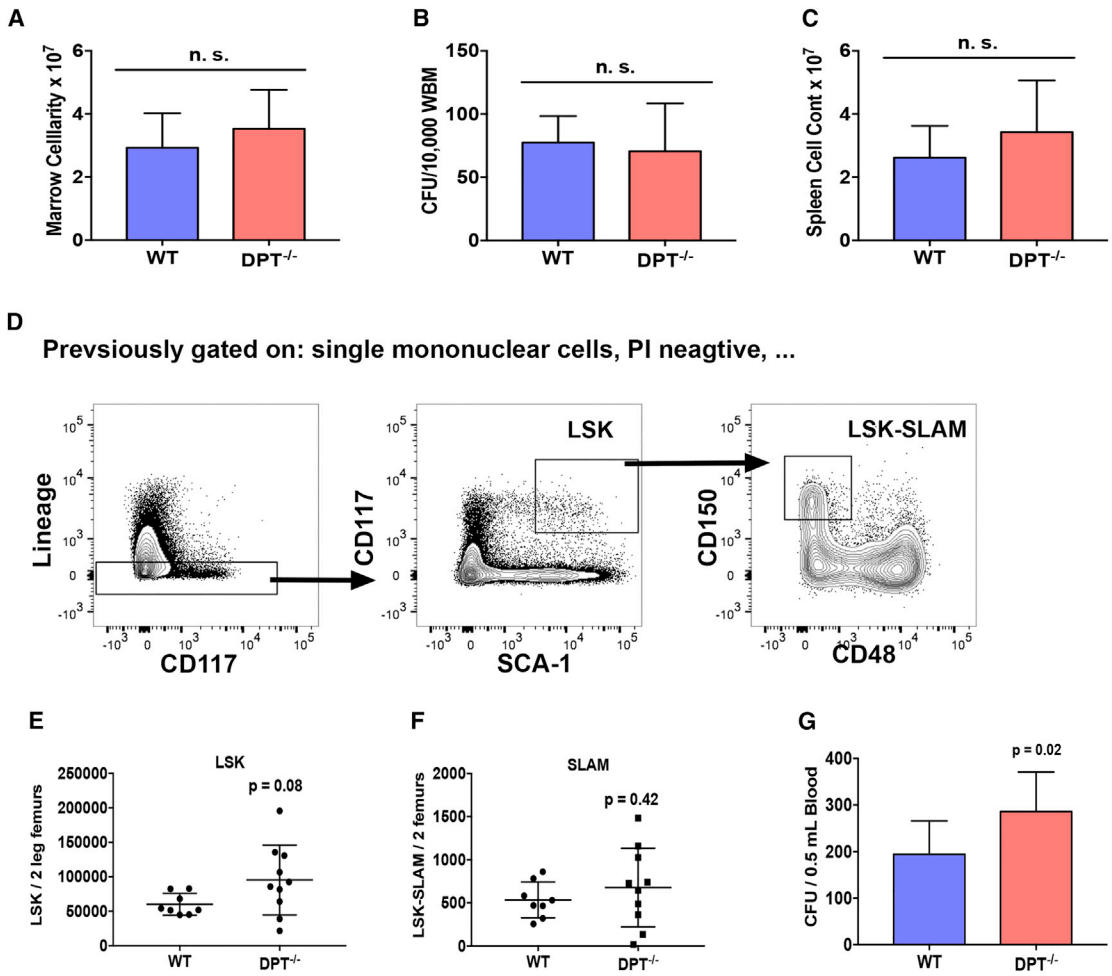

Figure 4. DTP Knockout Animals Have Normal Marrow HSPC and Increased Peripheral Mobilization

(A) Bone marrow cellularity of two femurs from 12-week-old mice (n = 10–12 individuals/group).

(B) CFU-C assay was performed using 10,000 WBM cells. CFU were enumerated after 12–14 days in culture (n = 10–12 individuals/group, each performed in triplicate).

(C) Spleen cellularity from 12-week-old mice (n = 10–12 individuals/group).

(D) Flow cytometry gating for bone marrow LSK and LSK-SLAM enumeration.

(E) Numbers of LSK performed on two femurs from 12-week-old mice (n = 8–10 individuals/group).

(F) Numbers of LSK-SLAM performed on two femurs from 12-week-old mice (n = 8–10 individuals/group).

(G) Peripheral blood CFU-C after AMD3100 induced HSPC mobilization (n = 10–12 individuals/group, each performed in triplicate).

All data are shown as means ± SD, p values from a Student's t test comparing experimental group with control. n.s., non-significant.

differences in hematopoietic nadir or recovery. We cannot exclude the possibly that DPT plays a more significant role in more specific situations, such as hematopoietic cell transplant. Interestingly, $DPT^{-/-}$ displayed an increased ability to mobilize CFU-C to the peripheral circulation after AMD3100 administration. This suggests that DPT can play a role in the retention of cells within the marrow microenvironment and its absence allows cells to mobilize more efficiently. Further exploration of this phenomenon is underway and will hopefully allow us to better understand the mechanism of DPT-related activity.

DPT has been demonstrated to interact with integrin family members such as ITGA3/ITGB1 (Liu et al., 2013; Okamoto et al., 2010). Okamoto et al. (2010) demonstrated that DPT can promote keratinocyte adhesion via a heparin sulfate proteoglycan-type receptor. The receptors for DPT on HSPC or OP9 cells remain unknown thus far, but an integrin family member is likely. Although our data suggest a role for DPT in *ex vivo* HSPC adherence, $DPT^{-/-}$ animals seem to have no overt hematopoietic defects. Given that the integrin family members as well as other adhesion promoting proteins are notoriously

promiscuous (Streuli and Akhtar, 2009), there may very well be other ECM proteins with overlapping functions working in concert with DPT.

EXPERIMENTAL PROCEDURES

All animal experiments were approved by the University of Minnesota Institutional Animal Care and Use Committee. Decellularization was performed on femurs split length-wise from three individual mice, as previously described, with the exception that each femur was placed in a well of a 6-well plate, and the decellularization solvents were added manually (Price et al., 2010).

Adherence Assay

A Millipore ECM Cell Adhesion Array Kit (ECM545) was used to measure WBM adherence to collagen (Col) species I–IV, laminin, tenascin, and vitronectin. After rehydration of wells, 150,000 freshly isolated murine WBM cells were plated in media in a total volume of 100 μL. rDPT was added at 2 μg/well. After 1 hr at 37°C, the wells were washed three times with 200 μL of assay buffer. Adhered cells were quantified using Lysis/CyQuant GR Dye solution on a fluorescent plate reader.

CFU-C Assay

CFU-C assays were performed using 10,000 WBM cells or 100 flow-sorted LSK (Lineage$^-$, SCA-1$^+$, KIT$^+$) cells using MethoCult GF M3434 (STEMCELL Technologies, Cambridge, MA) according to the manufacturer's instructions and read out after 14 days. Recombinant mDPT for this experiment, and all other experiments, was purchased from R&D Systems (5749-DP, Minneapolis, MN). In 5-FU experiments, mice were treated with a single dose of 5-FU delivered intraperitoneally 10 days prior to harvest.

rDPT Binding

rDPT or Fab′ fragment was covalently labeled with Alexa Fluor 488 using the Alexa Fluor 488 Protein Labeling Kit (Thermo Fisher Scientific, Waltham, MA) according to the manufacturer's instructions. Labeled rDPT was incubated with WBM at 1 μg/mL for 60 min on ice prior to washing twice with ice-cold PBS followed by analysis using flow cytometry.

In Vitro Expansion Assays

OP9 cells were grown to 80% confluence in a 96-well plate and irradiated at 3,000 Gy 1 day prior to LSK seeding. One hundred LSK cells were sorted by flow cytometry into each well of the 96-well plate containing StemSpan SFEM (STEMCELL Technologies), 100 ng/mL mSCF, 100 ng/mL mTPO, 100 ng/mL hFlt3, 100 ng/mL hIL6, and 10 ng/mL hIL11 ± 2 μg/mL rDPT for 5 days. In some experiments, there was no stroma layer, and cells were cultured directly on plastic. The hematopoietic cells in suspension above the stroma were carefully removed by gently pipetting and enumerated by flow cytometry. For experiments involving heparin, 10 USP units/mL of heparin (Sagent Pharmaceuticals, Schaumburg, IL) was added to each well during the culture period. Similarly, those cells adhered to the stroma were enumerated by flow cytometry using CountBright (Thermo Fisher Scientific) counting beads and anti-CD45 staining to allow isolation of only the hematopoietic cells.

For assessment of homing ability following *in vitro* expansion, CD45.2 lineage depleted WBM cells were sorted for viable LSK into a 96-well plate containing 100 μL of expansion medium (±DPT at 4 μg/mL). One hundred LSK cells were sorted into each well, then expanded for 5 days as above. CD45.1 recipient mice were irradiated at 9 Gy, 24 hr prior to transplant. Each mouse received the combined contents from six wells of expanded LSK cells (supernatant plus one PBS wash of stroma). Sixteen hours post transplant, femurs were harvested, and homed donor cells were assessed by flow cytometry as previously described (Astuti et al., 2017).

Generation of *Dpt* Knockout Mice

Disruption of murine *Dpt* was made by modification of mouse zygotes at the single-cell stage by pronuclear microinjection of two independent gRNAs targeting the first coding exon of the murine *Dpt* gene that were designed using the MIT CRISPR design tool (http://crispr.mit.edu/). *In vitro* transcribed gRNAs were produced using the MEGAshortscript T7 Transcription kit (Thermo Fisher Scientific) according to the manufacturer's protocols. Cas9 mRNA for microinjection was obtained from TriLink Biotechnologies (San Diego, CA). Founders were assessed using Surveyor assays followed by Sanger sequencing to detect mutations (Qiu et al., 2004).

Western Blot

Ten microliters of murine plasma from WT, DPT$^{+/-}$, DPT$^{-/-}$ mice using 1:500 anti-mDPT (Abcam, ab118710), followed by1:5,000 IgG-horseradish peroxidase (Cell Signaling Technology, Danvers, MA). Blot development was performed using the SuperSignal West Pico Chemiluminescent Substrate (Thermo Fisher).

Flow Cytometry

Peripheral blood and marrow flow cytometry methods and antibody list can be found in the Supplemental Experimental Procedures.

AMD3100 Mobilization

Wild-type and DPT$^{-/-}$ mice received 3 mg/kg AMD3100 (Sigma Chemical) via tail vein injection. One hour after AMD3100 administration, mice were killed via carbon dioxide asphyxiation, and 0.5 mL of whole blood was withdrawn by cardiac puncture. Whole blood was lineage depleted using the EasySep Mouse Hematopoietic Progenitor Cell Isolation Kit according to the manufacturer's instructions (STEMCELL Technologies). To perform CFU-C assays, lineage-negative cells were cultured on MethoCult GF M3434 (STEMCELL Technologies) according to the manufacturer's instructions and read out after 10–14 days.

SUPPLEMENTAL INFORMATION

Supplemental Information includes Supplemental Experimental Procedures, one figure, and two tables and can be found with this article online at http://dx.doi.org/10.1016/j.stemcr.2017.07.021.

AUTHOR CONTRIBUTIONS

A.C.K. edited the manuscript and performed cellular adhesion assays, A.L.B. and M.E.T. performed the analyses on the knockout mice, M.L. performed cellular adhesion assays, B.R.W. designed the CRISPRs for the knockout mice, and T.C.L. authored the initial and final drafts of the manuscript and oversaw the project.

ACKNOWLEDGMENTS

We gratefully acknowledge the Mouse Genetics Core Facility at the University of Minnesota Cancer Center. T.C.L. had grant support from the National Heart, Lung, and Blood Institute (K08HL108998, R03HL133318), the American Association of Blood Banks/National Blood Foundation, Regenerative Medicine Minnesota, and an American Society of Hematology Scholar Award. B.R.W. had support from the National Heart, Lung, and Blood Institute (T32-HL007062).

Received: February 7, 2017
Revised: July 25, 2017
Accepted: July 26, 2017
Published: August 24, 2017

REFERENCES

Astuti, Y., Kramer, A.C., Blake, A.L., Blazar, B.R., Tolar, J., Taisto, M.E., and Lund, T.C. (2017). A functional bioluminescent zebrafish screen for enhancing hematopoietic cell homing. Stem Cell Reports *8*, 177–190.

Forsberg, E., Hirsch, E., Frohlich, L., Meyer, M., Ekblom, P., Aszodi, A., Werner, S., and Fassler, R. (1996). Skin wounds and severed nerves heal normally in mice lacking tenascin-C. Proc. Natl. Acad. Sci. USA *93*, 6594–6599.

Grzegorzewski, K., Ruscetti, F.W., Usui, N., Damia, G., Longo, D.L., Carlino, J.A., Keller, J.R., and Wiltrout, R.H. (1994). Recombinant transforming growth factor beta 1 and beta 2 protect mice from acutely lethal doses of 5-fluorouracil and doxorubicin. J. Exp. Med. *180*, 1047–1057.

Hassan, H.T., Sadovinkova, E., Drize, N.J., Zander, A.R., and Neth, R. (1997). Fibronectin increases both non-adherent cells and CFU-GM while collagen increases adherent cells in human normal long-term bone marrow cultures. Haematologia (Budap) *28*, 77–84.

Klein, G., Beck, S., and Muller, C.A. (1993). Tenascin is a cytoadhesive extracellular matrix component of the human hematopoietic microenvironment. J. Cell Biol. *123*, 1027–1035.

Kokkaliaris, K.D., Drew, E., Endele, M., Loeffler, D., Hoppe, P.S., Hilsenbeck, O., Schauberger, B., Hinzen, C., Skylaki, S., Theodorou, M., et al. (2016). Identification of factors promoting ex vivo maintenance of mouse hematopoietic stem cells by long-term single-cell quantification. Blood *128*, 1181–1192.

Liu, X., Meng, L., Shi, Q., Liu, S., Cui, C., Hu, S., and Wei, Y. (2013). Dermatopontin promotes adhesion, spreading and migration of cardiac fibroblasts in vitro. Matrix Biol. *32*, 23–31.

Nakamura-Ishizu, A., Okuno, Y., Omatsu, Y., Okabe, K., Morimoto, J., Uede, T., Nagasawa, T., Suda, T., and Kubota, Y. (2012). Extracellular matrix protein tenascin-C is required in the bone marrow microenvironment primed for hematopoietic regeneration. Blood *119*, 5429–5437.

Nakano, T., Kodama, H., and Honjo, T. (1994). Generation of lymphohematopoietic cells from embryonic stem cells in culture. Science *265*, 1098–1101.

Ohta, M., Sakai, T., Saga, Y., Aizawa, S., and Saito, M. (1998). Suppression of hematopoietic activity in tenascin-C-deficient mice. Blood *91*, 4074–4083.

Okamoto, O., Suzuki, Y., Kimura, S., and Shinkai, H. (1996). Extracellular matrix 22-kDa protein interacts with decorin core protein and is expressed in cutaneous fibrosis. J. Biochem. *119*, 106–114.

Okamoto, O., Fujiwara, S., Abe, M., and Sato, Y. (1999). Dermatopontin interacts with transforming growth factor beta and enhances its biological activity. Biochem. J. *337* (Pt 3), 537–541.

Okamoto, O., Hozumi, K., Katagiri, F., Takahashi, N., Sumiyoshi, H., Matsuo, N., Yoshioka, H., Nomizu, M., and Fujiwara, S. (2010). Dermatopontin promotes epidermal keratinocyte adhesion via alpha3beta1 integrin and a proteoglycan receptor. Biochemistry *49*, 147–155.

Price, A.P., England, K.A., Matson, A.M., Blazar, B.R., and Panoskaltsis-Mortari, A. (2010). Development of a decellularized lung bioreactor system for bioengineering the lung: the matrix reloaded. Tissue Eng. Part A *16*, 2581–2591.

Qiu, P., Shandilya, H., D'Alessio, J.M., O'Connor, K., Durocher, J., and Gerard, G.F. (2004). Mutation detection using Surveyor nuclease. Biotechniques *36*, 702–707.

Seiffert, D. (1996). Detection of vitronectin in mineralized bone matrix. J. Histochem. Cytochem. *44*, 275–280.

Streuli, C.H., and Akhtar, N. (2009). Signal co-operation between integrins and other receptor systems. Biochem. J. *418*, 491–506.

Superti-Furga, A., Rocchi, M., Schafer, B.W., and Gitzelmann, R. (1993). Complementary DNA sequence and chromosomal mapping of a human proteoglycan-binding cell-adhesion protein (dermatopontin). Genomics *17*, 463–467.

Takeda, U., Utani, A., Wu, J., Adachi, E., Koseki, H., Taniguchi, M., Matsumoto, T., Ohashi, T., Sato, M., and Shinkai, H. (2002). Targeted disruption of dermatopontin causes abnormal collagen fibrillogenesis. J. Invest. Dermatol. *119*, 678–683.

Weinstein, R., Riordan, M.A., Wenc, K., Kreczko, S., Zhou, M., and Dainiak, N. (1989). Dual role of fibronectin in hematopoietic differentiation. Blood *73*, 111–116.

Wu, W., Okamoto, O., Kato, A., Matsuo, N., Nomizu, M., Yoshioka, H., and Fujiwara, S. (2014). Dermatopontin regulates fibrin formation and its biological activity. J. Invest. Dermatol. *134*, 256–263.

Yokota, T., Oritani, K., Takahashi, I., Ishikawa, J., Matsuyama, A., Ouchi, N., Kihara, S., Funahashi, T., Tenner, A.J., Tomiyama, Y., et al. (2000). Adiponectin, a new member of the family of soluble defense collagens, negatively regulates the growth of myelomonocytic progenitors and the functions of macrophages. Blood *96*, 1723–1732.

Yoshida, H., Hayashi, S., Kunisada, T., Ogawa, M., Nishikawa, S., Okamura, H., Sudo, T., Shultz, L.D., and Nishikawa, S. (1990). The murine mutation osteopetrosis is in the coding region of the macrophage colony stimulating factor gene. Nature *345*, 442–444.